Table VII. Vibrational and Structural Data for the Model Complexes *cis*-$[N_4Ru^{II}Cl_2]$ and *cis*-$[N_4Ru^{III}Cl_2]^+$

Ru–L	Δd,[a,b] Å	$\hbar\omega_{a_1}$, cm^{-1}	M_2, amu	Δ(Ru–L), Å
$Ru^{II/III}$–Cl	0.101	364	35.5	2.80
$Ru^{II/III}$–N_c	−0.037	400	80	1.61
$Ru^{II/III}$–N_t	−0.006	400	80	0.26

[a] From Table VI. [b] $\Delta Q_j = N^{1/2}|\Delta d_j|$, where N is the number of Ru–L bonds and Δd is the change in bond distance between oxidation states.

will employ the reduced force constant approach of Sutin.[48] For our treatment, this translates to a reduced symmetric stretch, $\hbar\omega_{a_1}(Ru^{II/III}–Cl)$, given by eq 5.

$$\hbar\omega_{a_1}(Ru^{II/III}–Cl) = \left[\frac{2(\hbar\omega_{a_1}(Ru^{II}–Cl))(\hbar\omega_{a_1}(Ru^{III}–Cl))}{(\hbar\omega_{a_1}(Ru^{II}–Cl))^2 + \hbar\omega_{a_1}(Ru^{III}–Cl))^2}\right]^{1/2} \quad (5)$$

The relevant vibrational and structural data needed to calculate λ_i are summarized in Table VII. From eq 2 and 4, λ_i for thermal electron transfer is given by

$$\lambda_i = \tfrac{1}{2}[2\hbar\omega_{a_1}(Ru^{II/III}–Cl)\,\Delta(Ru^{II/III}–Cl)^2 + 2\hbar\omega_{a_1}(Ru^{II/III}–N_c)\,\Delta(Ru^{II/III}–N_c)^2 + 2\hbar\omega_{a_1}(Ru^{II/III}–N_t)\,\Delta(Ru^{II/III}–N_t)^2] \quad (6)$$

Substituting the values in Table VII into eq 6 yields $\lambda_i = 3920$ cm^{-1}. Therefore, in the classical limit, the vibrational barrier to electron transfer from intramolecular modes is given by $\lambda_i/4 = 980$ cm^{-1}.

In fact, the classical limit relies on the assumption that $\hbar\omega << k_BT$. However, for metal–ligand vibrations at room temperature ($k_BT = 208.5$ cm^{-1} at 25 °C) the classical assumption is clearly inappropriate, and it is important to consider the full quantum treatment. Although our analysis has yielded the necessary parameters to carry out a complete vibrational overlap calculation,[11,12] for self-exchange reactions, the complete result is approximated accurately by eq 7.[10,48] Using the data in Table VII

$$\lambda_{i,QM} = \tfrac{1}{2}\sum_j \hbar\omega_j\Delta_j^2 \frac{4k_BT}{\hbar\omega_j}\tanh\frac{\hbar\omega_j}{4k_BT} \quad (7)$$

gives $\lambda_{i,QM} = 3680$ cm^{-1}, which is in good agreement with the classical value of $\lambda_i = 3920$ cm^{-1}. Our calculations reinforce those made earlier on other metal complexes, which show that at room temperature the classical approximation is adequate to calculate λ_i when vibrational trapping has its origin in low-frequency metal–ligand modes.

Final Comments. The analysis presented here has made an attempt to utilize the results of structural and vibrational analysis to define the intramolecular vibrational barrier to electron transfer for the couple $[Ru(bpy)_2Cl_2]^{+/0}$. Although the results are of interest in their own right, we will return to them later in an attempt to account for the optical electron-transfer properties of related mixed-valence dimers in a detailed way.

Acknowledgment is made to the Army Research Office under Grant No. DAAG29-82-K-0111 for support of this research.

Registry No. *cis*-$[Ru(bpy)_2Cl_2]\cdot 3.5H_2O$, 98014-14-3; *cis*-$[Ru(bpy)_2Cl_2]Cl\cdot 2H_2O$, 98014-15-4.

Supplementary Material Available: Tables of hydrogen atom parameters, thermal parameters, interatomic distances and angles, and values of $10F_o$ and $10F_c$ for *cis*-$[Ru(bpy)_2Cl_2]\cdot 3.5H_2O$ and *cis*-$[Ru(bpy)_2Cl_2]Cl\cdot H_2O$ (38 pages). Ordering information is given on any current masthead page.

(51) Jezowska-Trzebiatowska, B.; Hanuza, J. *J. Mol. Struct.* **1973**, *19*, 109.

Contribution from the Department of Chemistry, University of Virginia, Charlottesville, Virginia 22901

2,2′-Bipyrimidine-Bridged Homobinuclear Complexes

Greg Brewer and Ekk Sinn*

Received November 14, 1984

The synthesis and structural and magnetic properties of a series of 2,2′-bipyrimidine- (Bpm-) bridged binuclear complexes $L_2M(Bpm)ML_2$ of Mn(II), Co(II), and Ni(II) are reported, where L = $F_3CC(O)CHC(O)CF_3$ (hfa), $F_3CC(O)CHC(O)CH_3$ (tfa), and $F_3CC(O)CHC(O)C_6H_5$ (Phtfa). Mass spectroscopic observation of the $[ML_2(Bpm)]^+$ or $[ML_2(Bpm) - F]^+$ ions distinguishes the binuclear complexes from the mononuclear adducts. The complexes all exhibit antiferromagnetic exchange with a maximum in the magnetic susceptibility in the 18–23 K region for the Ni(II) complexes and in the 13–16 K region for the Co(II) complexes with L = tfa and Phtfa. The structure of one of the complexes, $(hfa)_2Co(Bpm)Co(hfa)_2$, is reported. It is monoclinic, $P2_1/n$, with $Z = 2$, $a = 8.790$ (3) Å, $b = 17.980$ (4) Å, $c = 12.490$ (6) Å, and $\beta = 102.76$ (3)°. The structure was refined to a R value of 4.9%. The two equivalent cobalt atoms are each bound to four hfa oxygens and two cis nitrogens of the Bpm in a slightly distorted octahedral environment. The cobalt atoms are 0.09 Å out of the Bpm plane, which provides favorable overlap of the metal $d_{x^2-y^2}$ orbitals with the ligand π system, allowing magnetic exchange to occur. The metal–metal separation is 5.750 (2) Å, the cobalt–oxygen bonds average 2.051 Å, and the cobalt–nitrogen bonds are 2.150 (3) Å.

Introduction

There has been great interest in the area of binuclear transition-metal complexes in recent years.[1-5] In part this stems from the fact that binuclear complexes have been found to occur in a number of metalloenzymes.[6] The influence of structure on magnetism of synthetic binuclear complexes is useful in assessing structurally unknown systems. Also of interest are the structural and electronic factors that contribute to the magnetic exchange interactions.

Homobinuclear complexes are more common than heterobinuclear ones and have been studied to a greater extent. Homobinuclear complexes can be symmetric, having identical donor atoms for each metal, or asymmetric arising from nonequivalent donor sets (e.g. **1**) or by accidental addition of a monodentate ligand to one of two equivalent donor sets[7] (**2**). Symmetric complexes occur in some salts such as copper acetate,[8] $[Cu(R\text{-}sal)Cl]_2$ (**3**), and $[Ni(R\text{-}sal)NO_3L]_2$[10] (**4**) (L = solvent), or they

(1) (a) Gruber, S. J.; Harris, C. M.; Sinn, E. *Inorg. Chem.* **1968**, *7*, 268. (b) *Ibid. J. Inorg. Nucl. Chem.* **1968**, *30*, 1805.
(2) Castello, U.; Vigato, P. A.; Viladi, M. *Coord. Chem. Rev.* **1977**, *23*, 31.
(3) Sinn, E.; Harris, C. M. *Coord. Chem. Rev.* **1969**, *4*, 391.
(4) Hodgson, D. P. *Prog. Inorg. Chem.* **1974**, *19*, 173.
(5) Krautil, P.; Robson, R. J. *Coord. Chem.* **1980**, *10*, 7.
(6) Kurtz, D. M., Jr.; Shriver, D.; Klotz, I. M. *Coord. Chem. Rev.* **1977**, *24*, 145.
(7) Butcher, R. J.; Devan, G.; Mockler, G. M.; Sinn, E., submitted for publication.
(8) Van Niekerk, J. H.; Schoenig, F. R. L. *Acta Crystallogr.* **1953**, *6*, 227. De Meester, P.; Fletcher, S. R.; Skapski, A. C. *J. Chem. Soc., Dalton Trans.* **1973**, 2575.

0020-1669/85/1324-4580$01.50/0

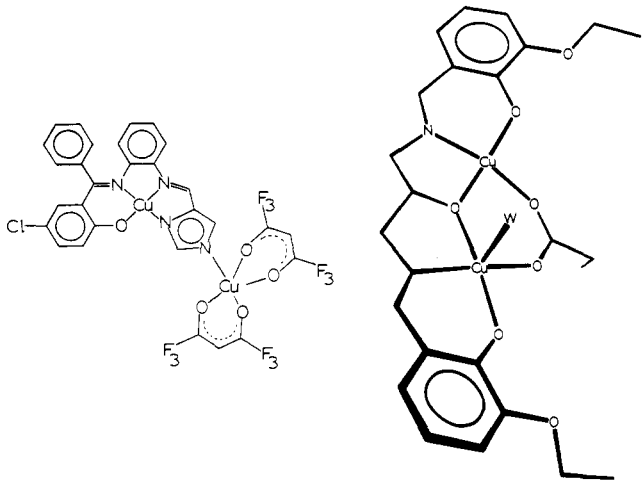

1 2

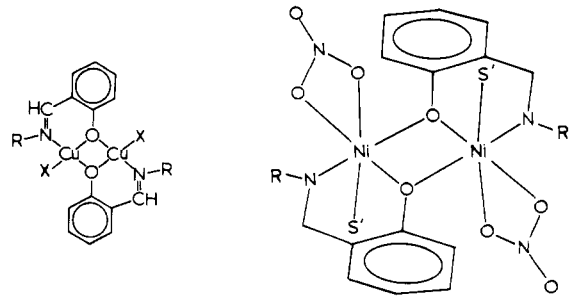

3 4

can be formed by the action of a binucleating ligand. Complexes of this type allow observation of magnetic exchange interactions with a range of metals in a similar structural environment to be made.

Symmetric binucleating ligands include pyrazine, pyz (**5**), 2,2′-biimidazole, Biim (**6**), and 2,2′-bipyrimidine, Bpm (**7**). There

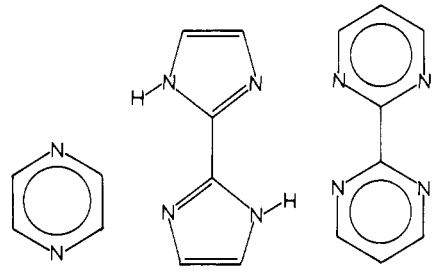

5 6 7

are reports of pyrazine bridging in $[Cu(hfa)(pyz)]_2$[11] and $[VO(hfa)_2]_2(pyz)$.[12] Biim and tetracyanobiimidazole, Tcbiim, serve as bridges in $[Cu(diethylenetriamine)]_2(Biim)(BF_4)_2$[13] and $Ir_2(1,5\text{-cyclooctadiene})_2(Tcbiim)$.[14] There are reports of Bpm serving as a homobinuclear bridge with manganese[15] in $Cl_2Mn(Bpm)MnCl_2$, with platinum[15] in $(C_6H_6)_2Pt(Bpm)Pt(C_6H_6)_2$, with ruthenium[16] in $(bpy)_2Ru(Bpm)Ru(bpy)_2$ (bpy = 2,2′-bipyridine), with copper[17] in $(hfa)_2Cu(Bpm)Cu(hfa)_2$, and with molybdenum, chromium, or tungsten[18] in $(CO)_4M(Bpm)M(CO)_4$. There are a few reports of Bpm serving as a heterobinuclear bridge in $(CO)_4Mo(Bpm)M(CO)_4$[18] (M = Cr, W) and with platinum and manganese[15] in $(C_6H_6)_2Pt(Bpm)MnCl_2$. A cytochrome *c* oxidase model that was postulated[17] to have a Bpm bridge between a iron(II) and copper(II) was recently shown not to have the metals linked by a Bpm bridge.[19]

We report the magnetic properties and structure of a series of symmetric binuclear complexes with Bpm of the type $L_2M(Bpm)ML_2$, where M = Ni, Co, or Mn, L = $F_3CC(O)CHC(O)R$, and R = CF_3 (hfa), CH_3 (tfa), or C_6H_5 (Phtfa). This is the first report of magnetic and structural data on a Bpm-bridged binuclear system.

Experimental Section

General Information. The substituted metal acetylacetonates were prepared by the standard procedures.[20] $Fe(hfa)_2$ was prepared by the method of Buckingham.[21] 2-Bromopyrimidine, used to obtain Bpm, was obtained from 2-aminopyrimidine by the method of Bly.[22] Bpm was obtained by the action of copper bronze on 2-bromopyrimidine by a modification[19] of the literature method. Elemental analyses were conducted by Galbraith Laboratories. Mass spectra were obtained on a conventional electron-impact instrument.

Synthesis. Mononuclear adducts of the type $M(hfa)_2(Bpm)$ were prepared by mixing the reagents in a 1:1 fashion in methanol. The binuclear complexes $L_2M(Bpm)ML_2$ were prepared by adding 0.1 mmol of Bpm to 0.2 mmol of ML_2 in a minimum volume of methanol. The binuclear complexes precipitated in 24–48 h.

Magnetism. The magnetic susceptibilities (4–110 K) were recorded on a SQUID magnetometer. The calibration and method of operation are as described.[23,24]

Crystal Data: $(hfa)_2Co(Bpm)Co(hfa)_2$, $Co_2F_{24}O_8N_4C_{28}H_{10}$, mol wt 1104, space group $P2_1/n$, $Z = 2$, $a = 8.790$ (3) Å, $b = 17.980$ (4) Å, $c = 12.490$ (6) Å, $\beta = 102.76$ (3)°, $V = 1925$ Å^3, ρ(calcd) = 1.91 g cm^{-3}, ρ(obsd) = 1.88 g cm^{-3}, μ(Mo Kα) = 10.8 cm^{-1}; crystal dimensions (distances in mm of faces from centroid) (100) 0.27, ($\bar{1}$00) 0.27, (011) 0.06, (0$\bar{1}\bar{1}$) 0.06), (01$\bar{1}$) 0.14, (0$\bar{1}$1) 0.14; maximum and minimum transmission coefficients 0.89 and 0.78.

Data Collection. Cell dimensions and space group data were obtained by the standard methods on an Enraf-Nonius four-circle CAD-4 diffractometer. The θ–2θ scan technique was used as described previously[25] to record the intensities for all nonequivalent reflections for which $1° < 2\theta < 48°$. Scan widths were calculated as $(A + B \tan \theta)$, where A is estimated from the mosaicity of the crystal and B allows for the increase in peak width due to $K\alpha_1 - K\alpha_2$ splitting. The values of A and B were 0.60 and 0.35°, respectively; $\lambda = 0.7107$ Å for $+h,+k,\pm l$ collected at 290 K.

The intensities of four standard reflections showed no greater fluctuations during data collection (2.1%) than those expected from Poisson statistics. The raw intensity data were corrected for Lorentz–polarization effects and absorption. Of the 2550 independent intensities for $(hfa)_2Co(Bpm)Co(hfa)_2$ there were 1998 with $F_o^2 > 3\sigma(F_o^2)$, where $\sigma(F_o^2)$ was estimated from counting statistics.[26] These data were used in the final refinement of the structural parameters.

Structure Determination. A three-dimensional Patterson function was used to determine the metal positions, which phased the intensity data sufficiently well to permit location of the other non-hydrogen atoms from Fourier synthesis. Full-matrix least-squares refinement was carried out as previously described.[25] Anisotropic temperature factors were introduced for all non-hydrogen atoms. Further Fourier difference functions permitted location of the hydrogen atoms, which were included in the refinement for three cycles of least squares and then held fixed. $(hfa)_2Co(Bpm)Co(hfa)_2$ converged with $R = 4.9\%$ and $R_w = 5.4\%$. A

(9) Countryman, R. M.; Robinson, W. T.; Sinn, E. *Inorg. Chem.* **1974**, *13*, 2013.
(10) Jasinski, J.; Butcher, R. J.; Mockler, G. M.; Sinn, E. *J. Chem. Soc., Dalton Trans.* **1976**, 1059.
(11) Belford, R. C. E.; Foster, D. E.; Truter, M. R. *J. Chem. Soc., Dalton Trans.* **1974**, 17.
(12) Haddad, M. S.; Hendrickson, D. N.; Cannady, J. P.; Drago, R. S.; Bieksza, D. *J. Am. Chem. Soc.* **1974**, *101*, 898.
(13) Haddad, M. S.; Hendrickson, D. N. *Inorg. Chem.* **1978**, *17*, 2622.
(14) Rasmussen, P. G.; Bailey, O. H.; Bayon, T. C. Inorg. *Chem.* **1984**, *23*, 338.
(15) Lonxa, S. *Inorg. Chim. Acta* **1983**, *75*, 131.
(16) (a) Hunziker, M.; Ludi, A. *J. Am. Chem. Soc.* **1977**, *99*, 7370. (b) Dose, E. V.; Wilson, L. J. *Inorg. Chem.* **1978**, *17*, 2660.
(17) Petty, R. H.; Welch, B. R.; Wilson, L. J.; Bottomley, L. A.; Kadish, K. M. *J. Am. Chem. Soc.* **1980**, *102*, 611.
(18) Overton, C.; Connor, J. A. *Polyhedron* **1982**, *1*, 53.
(19) Brewer, G.; Sinn, E. *Inorg. Chem.* **1984**, *23*, 2532.
(20) (a) Cotton, F. A.; Holm, R. H. *J. Am. Chem. Soc.* **1960**, *82*, 2979. (b) Walker, W. R.; Li, N. C. *J. Inorg. Nucl. Chem.* **1965**, *27*, 2255.
(21) Buckingham, D. A.; Gorges, R. C.; Henry, J. T. *Aust. J. Chem.* **1967**, *20*, 281.
(22) Bly, D. B.; Mellor, M. G. *J. Org. Chem.* **1962**, *27*, 2945.
(23) O'Connor, C. J.; Sinn, E.; Cukauskas, E. J.; Deaver, B. S. *Inorg. Chim. Acta* **1979**, *32*, 29.
(24) O'Connor, C. J.; Sinn, E.; Deaver, B. S. *J. Chem. Phys.* **1979**, *70*, 5161.
(25) Freyberg, D. P.; Mockler, G. M.; Sinn, E. *J. Chem. Soc., Dalton Trans.* **1976**, 447.
(26) Corfield, P. W. R.; Doedens, R. J.; Ibers, J. A. *Inorg. Chem.* **1967**, *6*, 197.

final Fourier difference function was featureless, with peaks of less than 0.3 e/Å^3 near the Co atoms. Tables of observed and calculated structure factors and thermal parameters are available as supplementary material. The principal programs used are as described previously.[25]

Results and Discussion

Synthesis. The mononuclear and binuclear complexes were easily prepared by the reaction of the metal acetylacetonates and Bpm in a 1:1 or 2:1 stoichiometry respectively. $Mn(tfa)_2$, $Mn(hfa)_2$, and $Fe(hfa)_2$ yielded only the mononuclear products, $ML_2(Bpm)$, by this simple procedure. These complexes were identified as being mononuclear on comparison of their magnetic properties and melting points with authentic samples of the mononuclear materials prepared by the 1:1 reaction. Altering the stoichiometry from 2:1 to 2.5:1 produced no effect. The manganese binuclear adducts may have formed by this procedure but were not isolated due to solubility. $Mn(Phtfa)_2$ did however binucleate with Bpm. The inability to isolate a binuclear complex with $Fe(hfa)_2$ may have been caused by unfavorable solubility properties or oxidative decomposition. The ability of Bpm to bind to iron was demonstrated by the formation of the mononuclear complex, $Fe(hfa)_2(Bpm)$. The reaction of other iron acetylacetonates was not investigated because these complexes are even more sensitive to oxidation. The 1400-cm^{-1} ring stretching mode of free Bpm was observed to shift to higher frequency on formation of either the mono- or binuclear products.[18] Attempts to form mixed-metal species, $L_2M(Bpm)M'L_2$, by this simple reaction resulted in the isolation of $L_2M(Bpm)ML_2$ and $L_2M'(Bpm)M'L_2$. In the case of the $Cu(hfa)_2$ and $Fe(hfa)_2$ reactions the products were $(hfa)_2Cu(Bpm)Cu(hfa)_2$ and $Fe(hfa)_2Bpm$. The products were identified by comparison of melting points and mass spectra with those of authentic samples following visible separation of the differently colored complexes.

Mass Spectra. Our results show that the mass spectra can be used as excellent criteria for the formation of mono- and binuclear complexes. All the complexes produce ions characteristic of the metal acetylacetonate including the $[ML_2]^+$, $[ML_2 - CF_3]^+$, and $[ML - CF_2]^+$ peaks.[27] In addition to these peaks there are the $[ML_2(Bpm)]^+$, $[ML_2(Bpm) - F]^+$, $[ML(Bpm)]^+$, and $[MF(Bpm)]^+$ ions,[28] which incorporate the Bpm nucleus. The parent ion, $[L_2M(Bpm)ML_2]^+$, is never observed, presumably because of its instability under the conditions employed. The $(Phtfa)_2Ni(Bpm)Ni(phtfa)_2$ and $(hfa)_2Co(Bpm)Co(hfa)_2$ complexes exhibit low-intensity binuclear ions of the type $[L_2M(Bpm)M]^+$. Under milder ionization conditions it may be possible to observe the $[L_2M(Bpm)ML]^+$ or parent $[L_2M(Bpm)ML_2]^+$ ions. All the binuclear complexes studied exhibit a $[ML_2(Bpm)]^+$ or $[ML_2(bpm) - F]^+$ ion, which distinguishes them from the mononuclear complexes that lack this feature. The mixed fragment ions $[ML(Bpm)]^+$ and $[MF(Bpm)]^+$ illustrate the strength of the Bpm chelate. The molecule undergoes loss of a negatively charged ligand under fragmentation rather than loss of a neutral one. The intensities of the $[ML(Bpm)]^+$ ion can be used as a guide to the strength of the bonding of L. In the hfa adducts the $[ML(Bpm)]^+$ ion was the base peak, with $[FM(Bpm)]^+$ as the next most intense peak. These ions shrink to only moderate intensity when L is tfa, and when L is Phtfa, the $[ML(Bpm)]^+$ ion becomes smaller still while $[MF(Bpm)]^+$ disappears entirely. This shows the loss of L becomes more difficult along the series $-CF_3$, $-CH_3$, $-Ph$. The loss of two Phtfa ligands becomes so difficult that it does not occur.

Structure. To date, the $(hfa)_2Co(Bpm)Co(hfa)_2$ molecule is the only Bpm-bridged binuclear complex characterized by a crystal structure. Table I gives the positional parameters. The bond distances and angles are given in Tables II and III, respectively. The digits in parentheses in the tables are the standard deviations in the least significant figures quoted, and they were derived from the inverse matrix in the course of least-squares refinement calculations. The halves of the molecule are related by a crystallographically imposed inversion center located halfway between the halves of the Bpm molecule. The metal to metal separation is 5.750 (2) Å. The geometry about the cobalt atom is only slightly distorted from that of a regular octahedron. The four cobalt to oxygen bonds average 2.051 Å, and the cobalt to nitrogen bonds are 2.150 Å. There is slight evidence of distortion along the O(1)–Co–N(1B) axis as the Co–O bond is lengthened from 2.048 Å in the other Co–O bonds to 2.058 Å. The molecule consists of well-separated discrete binuclear units. Figure 1 gives a stereoview of the molecule; a molecular packing diagram is available as supplementary materiai.

The three principal planes in the molecule consist of the Bpm plane and the two hfa planes. The cobalt atom lies 0.09 Å out

Table I. Positional Parameters for $(hfa)_2Co(Bpm)Co(hfa)_2$

atom	*x*	*y*	*z*
Co	0.26054 (9)	0.09510 (5)	0.08799 (6)
F(11)	0.3943 (6)	0.3262 (2)	0.2415 (3)
F(12)	0.2058 (6)	0.3640 (3)	0.1218 (5)
F(13)	0.4356 (6)	0.3791 (2)	0.1021 (4)
F(51)	0.4731 (5)	0.2415 (3)	−0.2170 (3)
F(52)	0.4159 (6)	0.1297 (3)	−0.2368 (3)
F(53)	0.2417 (6)	0.2133 (4)	−0.2750 (3)
F(61)	0.7988 (5)	0.1202 (3)	0.2463 (4)
F(62)	0.7742 (5)	0.0084 (3)	0.2127 (4)
F(63)	0.7961 (5)	0.0478 (3)	0.3749 (3)
F(101)	0.3592 (5)	0.0768 (3)	0.5202 (3)
F(102)	0.1380 (5)	0.0659 (4)	0.4310 (4)
F(103)	0.2425 (8)	0.1664 (3)	0.4441 (4)
O(1)	0.2842 (5)	0.2057 (2)	0.1310 (3)
O(2)	0.2997 (5)	0.1257 (2)	−0.0616 (3)
O(3)	0.4904 (4)	0.0694 (2)	0.1493 (3)
O(4)	0.2212 (4)	0.0800 (2)	0.2422 (3)
N(1B)	0.2055 (5)	−0.0176 (3)	0.0364 (4)
N(3B)	−0.0101 (5)	−0.0972 (3)	−0.0306 (3)
C(1)	0.3426 (8)	0.3325 (4)	0.1370 (6)
C(2)	0.3280 (7)	0.2571 (3)	0.0786 (5)
C(3)	0.3588 (7)	0.2536 (4)	−0.0267 (5)
C(4)	0.3389 (7)	0.1892 (3)	−0.0882 (5)
C(5)	0.3655 (8)	0.1934 (4)	−0.2063 (6)
C(6)	0.7303 (7)	0.0593 (4)	0.2728 (5)
C(7)	0.5553 (7)	0.0697 (3)	0.2493 (5)
C(8)	0.4863 (7)	0.0785 (3)	0.3384 (5)
C(9)	0.3260 (7)	0.0842 (3)	0.3264 (5)
C(10)	0.2646 (8)	0.0986 (4)	0.4313 (5)
C(2B)	0.0534 (6)	−0.0312 (3)	0.0018 (4)
C(4B)	0.0882 (7)	−0.1546 (3)	−0.0281 (5)
C(5B)	0.2458 (7)	−0.1457 (4)	0.0064 (5)
C(6B)	0.3017 (7)	−0.0758 (3)	0.0372 (5)
H(3)	0.403 (6)	0.299 (3)	−0.057 (4)
H(8)	0.551 (5)	0.082 (3)	0.411 (4)
H(4B)	0.041 (5)	−0.201 (3)	−0.055 (4)
H(5B)	0.314 (6)	−0.186 (3)	0.010 (4)
H(6B)	0.415 (6)	−0.069 (3)	0.064 (4)

Table II. Bond Distances (Å) for $(hfa)_2Co(Bpm)Co(hfa)_2$

Co–O(1)	2.058 (3)	Co–N(1B)	2.150 (3)
Co–O(2)	2.048 (3)	Co–N(3B)′	2.160 (3)
Co–O(3)	2.049 (3)	Co–Co′	5.750 (4)
Co–O(4)	2.049 (3)		

Table III. Selected Bond Angles (deg) for $(hfa)_2Co(Bpm)Co(hfa)_2$

O(1)–Co–O(2)	87.2 (1)	O(4)–Co–N(1B)	94.8 (1)
O(1)–Co–O(3)	94.9 (1)	O(4)–Co–N(3B)	86.7 (1)
O(1)–Co–O(4)	84.9 (1)	N(1B)–Co–N(3B)′	76.8 (1)
O(1)–Co–N(1B)	172.9 (1)	Co–O(1)–C(2)	127.4 (3)
O(1)–Co–N(3B)′	96.1 (1)	Co–O(2)–C(4)	126.6 (3)
O(2)–Co–O(3)	92.9 (1)	Co–O(3)–C(7)	124.5 (3)
O(2)–Co–O(4)	172.0 (1)	Co–O(4)–C(9)	122.7 (3)
O(2)–Co–N(1B)	93.0 (1)	Co–N(1B)–C(2B)	114.4 (3)
O(2)–Co–N(3B)′	93.3 (1)	Co–N(1B)–C(6B)	129.2 (3)
O(3)–Co–O(4)	88.6 (1)	Co–N(3B)′–C(2B)′	114.4 (3)
O(3)–Co–N(1B)	92.2 (1)	Co–N(3B)′–C(6B)′	128.8 (3)
O(3)–Co–N(3B)′	167.6 (1)		

(27) Reichert, C.; Bancroft, G. M.; Westmore, J. B. *Can. J. Chem.* **1970**, *48*, 1362.
(28) Izumi, F.; Kurosawa, R.; Kawamoto, H.; Akaiwa, H. *Bull. Chem. Soc. Jpn.* **1975**, *48*, 3188.

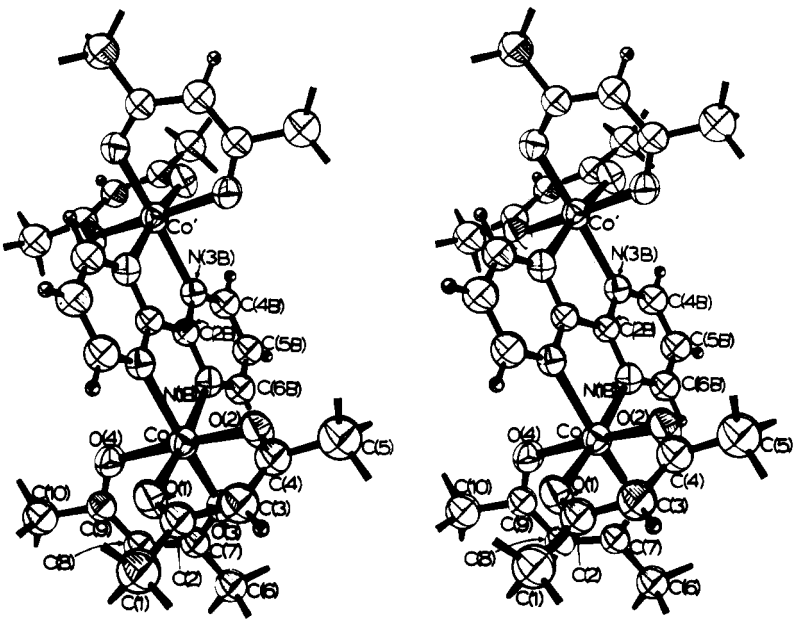

Figure 1. Stereoview of $(hfa)_2Co(Bpm)Co(hfa)_2$.

of the Bpm plane. This bridge should foster magnetic exchange, as there should be good overlap of the metal $d_{x^2-y^2}$ orbitals with the Bpm π system. The Bpm plane is at angles of 81.5 and 72.4° to the hfa planes. The hfa planes intersect at an angle of 81.1°.

The structure of the other six binuclear complexes should be similar. The Bpm should serve to hold the metals in a coplanar alignment, with the rest of the octahedron being made up of oxygens. One likely structural effect of changing L from hfa to tfa or Phtfa is increasing distortion of the pseudooctahedral metal environment as the ligand symmetry decreases. The four Co–O bonds in the present example are all nearly equal because hfa is symmetric. In the asymmetric ligands there may be long and short Co–O bonds due to the differences in electron-donating ability of the two oxygen atoms.

Magnetism. The mononuclear materials exhibit moments that agree well with the spin-only values. The binuclear complexes show considerable variation of magnetic moment with temperature, indicative of antiferromagnetic exchange between the metals. The nickel complexes and $(tfa)_2Co(Bpm)Co(tfa)_2$ and $(Phtfa)_2Co(Bpm)Co(Phtfa)_2$ show a maximum in the susceptibility in the 18–23 and 13–16 K regions, respectively.

The susceptibilities were analyzed in terms of the spin-only equation for homobinuclear complexes with an isotropic exchange interaction, $H = -2J\mathbf{S}_1\cdot\mathbf{S}_2$:

$$\chi = \frac{Ng^2\beta^2}{6kT}\frac{\sum_{i=0}^{2S-1}(2S-i)(2S-i+1)(4S-2i+1)y_i}{\sum_{i=0}^{2S}(4S+1-2i)y_i}$$

$$y = e^{i(i-4S-1)J/kT}$$

Least-squares analysis for $(hfa)_2Ni(Bpm)Ni(hfa)_2$ (Figure 2) yielded $-J = 5.8$ cm^{-1} and $g = 2.01$. The fit was only slightly improved by inclusion of zero-field splitting[29] with $-J = 6.5$ cm^{-1}, $g = 2.00$, and $D = 31$ cm^{-1}. $(tfa)_2Ni(Bpm)Ni(tfa)_2$ and $(Phtfa)_2Ni(Bpm)Ni(Phtfa)_2$ (Figure 2) have identical temperature points of maximum susceptibility and therefore identical $-J$ values. Analysis yielded $-J = 5.6$ cm^{-1} and $g = 2.13$ and 2.06, respectively. The former required $D = 41.8$ cm^{-1}. Similarly, $(tfa)_2Co(Bpm)Co(tfa)_2$ and $(Phtfa)_2Co(Bpm)Co(Phtfa)_2$ (Figure 3) have identical points of maximum susceptibility with $-J = 3.65$ cm^{-1} and $g = 2.68$ and 2.41, respectively. The manganese complex,

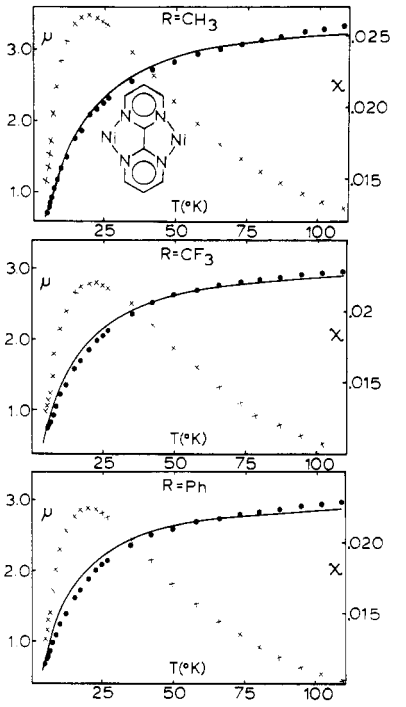

Figure 2. Magnetic moments (μ) and susceptibilities (χ) of $L_2Ni(Bpm)NiL_2$, where L = $RC(O)CHC(O)CF_3$. R = CH_3, CF_3, and Ph for L = tfa, hfa, and Phtfa, respectively.

Table IV. Coupling Parameters in $[RC(O)CHC(O)CF_3]M(Bpm)M[RC(O)CHC(O)CF_3]$

M	R	$-J$, cm^{-1}	$-JS^2$, cm^{-1}
Ni	CH_3	5.6	5.6
Ni	Ph	5.6	5.6
Ni	CF_3	6.5	6.5
Co	CF_3	3.5	7.9
Co	CH_3	3.7	8.2
Co	Ph	3.7	8.2
Mn	Ph	0.46	3.1

$(Phtfa)_2Mn(Bpm)Mn(Phtfa)_2$ (Figure 4), exhibits no susceptibility maximum above 4.3 K, but the decrease in moment with falling temperature indicates antiferromagnetic exchange with $-J = 0.5$ cm^{-1} and $g = 2.03$ (Table IV).

The extent of magnetic exchange in this series of five nickel and cobalt complexes is dependent on the metal but is independent

(29) Ginsberg, A. P.; Martin, R. L.; Brookes, R. W.; Sherwood, R. C. *Inorg. Chem.* **1972**, *11*, 2884.

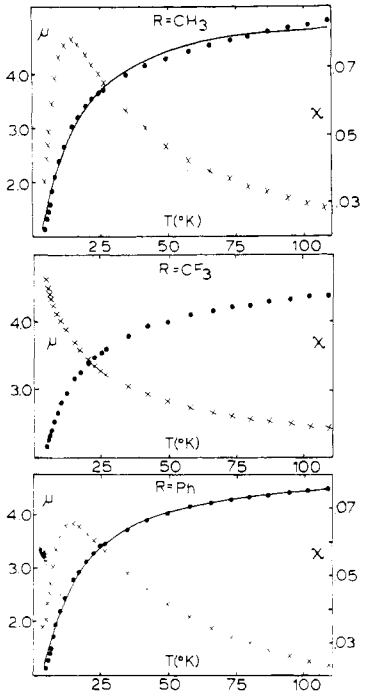

Figure 3. Magnetism of $[RC(O)CHC(O)CF_3]Co(Bpm)Co[RC(O)CHC(O)CF_3]$ (see Figure 2).

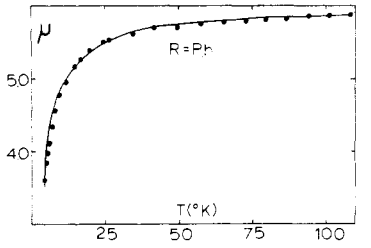

Figure 4. Magnetism of $(Phtfa)_2Mn(Bpm)Mn(Phtfa)_2$ (see Figure 2).

of whether L is tfa or Phtfa. Thus, the distortion caused by lowering the symmetry of L from hfa to tfa or Phtfa is much the same whether tfa or Phtfa is used. This suggests that similar N–M–N bond distances and angles are probably required for the relatively rigid Bpm.

The $(hfa)_2Co(Bpm)Co(hfa)_2$ complex differs from the other two cobalt complexes in that it does not exhibit a susceptibility maximum in the 13–16 K region. This difference in magnetic behavior is attributed to the only slightly distorted octahedral cobalt environment which should foster a ground state that corresponds reasonably closely to $^4T_1$. In this case, spin–orbit coupling is at least as important as the magnetic exchange and eliminates any susceptibility maximum above 4.3 K. In the other two cobalt complexes the asymmetry of the ligands must split the $^4T_1$ ground state by lowering the symmetry of the cobalt sufficiently to remove the orbital degeneracy and effectively eliminate the spin–orbit coupling. These complexes closely resemble the analogous nickel ones in which spin–orbit coupling is not present. The ligand to metal bond distances and angles for $(hfa)_2Co(Bpm)Co(hfa)_2$ do not show a great deal of deviation from what would be expected of a pure octahedron, which agrees well with the magnetic results. The other complexes must experience greater structural distortions, as is evidenced by the fact that their magnetic properties are largely described by the simple Heisenberg model.

The Bpm bridge has been shown to foster magnetic exchange in these homobinuclear complexes over a M–M separation of ~6 Å. This ability must certainly be linked to favorable overlap of the metal $d_{x^2-y^2}$ orbitals with the π framework of Bpm. The octahedral coordination of the metals and the steric requirements of Bpm combine to hold both metals in the Bpm plane. There is only a 0.09-Å deviation of the metal from the plane, which reduces the magnetic coupling below the maximum.

It is interesting to compare the magnetic properties of this series with other binucleating ligands. A series described by Hendrickson et al. utilizes a ligand derived from 2,6-diformyl-4-methylphenol.[30] This series is somewhat different from the present, as the metals pull out of the principal plane of the ligand due to their square-pyramidal geometry. Octahedral complexes, structurally closer to the present series, are prepared by the reaction of the above with pyridine.[31] The $-J$ values for all these binuclear complexes are given in Table IV. It is seen that the $-J$ values for the series derived from diformylphenol are greater than those given for Bpm. This must be attributed to the more efficient and stronger exchange pathways of the former. One feature that all the series have in common is a general reduction in $-J$ as M is varied from Cu(II) to Mn(II) in the M(II)–M(II) homobinuclear complexes. This reduction in $-J$ is probably attributable to electronic factors in this series, as structural variations with the relatively rigid Bpm complexes are expected to be less significant. The Mn(II)–Mn(II) couple was the weakest Bpm-bridged complex studied, but it still demonstrated net antiferromagnetic exchange. Hendrickson's Mn(II)–Mn(II) complex was weakly ferromagnetically coupled in contrast to the other members of the same series and the present complex. This reflects the delicate balance between ferro- and antiferromagnetic interactions in homobinuclear complexes. This is of particular importance in systems with a large number of unpaired d electrons as with Mn(II) (d^5), because there are an increasing number of ferromagnetic exchange pathways to consider.[32]

2,2′-Bipyrimidine (**7**) has been shown structurally to promote binucleation and is a fairly rigid bridge. In the seven binuclear complexes investigated magnetically it was shown that Bpm promoted antiferromagnetic exchange. Absence of exchange in a recently reported cytochrome *c* oxidase model containing Fe(II) and Cu(II)[17] provides further evidence[19] that the metals are not linked by a Bpm bridge.

Acknowledgment. Support under NSF Grants CHE83-00516 and CHE83-11449 is gratefully acknowledged.

Registry No. $(tfa)_2Ni(Bpm)Ni(tfa)_2$, 99354-86-6; $(Phtfa)_2Ni(Bpm)Ni(Phtfa)_2$, 99354-87-7; $(hfa)_2Ni(Bpm)Ni(hfa)_2$, 90886-36-5; $(hfa)_2Co(Bpm)Co(hfa)_2$, 90886-37-6; $(tfa)_2Co(Bpm)Co(tfa)_2$, 99354-88-8; $(Phtfa)_2Co(Bpm)Co(Phtfa)_2$, 99354-89-9; $(Phtfa)_2Mn(Bpm)Mn(Phtfa)_2$, 99354-90-2; $Mn(tfa)_2$, 20080-72-2; $Co(tfa)_2$, 47115-08-2; $Ni(tfa)_2$, 14324-83-5; $Mn(hfa)_2$, 19648-86-3; $Co(hfa)_2$, 19648-83-0; $Ni(hfa)_2$, 14949-69-0; $Fe(hfa)_2$, 28736-68-7; $Mn(Phtfa)_2$, 14052-09-6; $Co(Phtfa)_2$, 14052-08-5; $Ni(Phtfa)_2$, 14052-10-9.

Supplementary Material Available: Tables of thermal parameters, bond lengths and angles, and observed and calculated structure factors and a packing diagram (12 pp). Ordering information is given on any current masthead page.

(30) Lambert, S. L.; Hendrickson, D. N. *Inorg. Chem.* **1979**, *18*, 2683.
(31) Spiro, C. L.; Lambert, S. L.; Smith, T. J.; Duesler, E. N.; Gagne, R. R.; Hendrickson, D. N. *Inorg. Chem.* **1981**, *20*, 1229.
(32) Kahn, O.; Tola, P.; Coudanne, H. *Chem. Phys.* **1979**, *42*, 355.